

Multi-tap complex-coefficient incoherent microwave photonic filters based on optical single-sideband modulation and narrow band optical filtering

Mikel Sagues¹, Raimundo García Olcina², Alayn Loayssa¹, Salvador Sales², and José Capmany²

¹*Departamento de Ingeniería Eléctrica y Electrónica, Universidad Pública de Navarra
Campus Arrosadia s/n, 31006 Pamplona (Spain)*

²*Optical and Quantum Communications Group, iTEAM-Universidad Politécnica de Valencia
C/ Camino de Vera s/n, 46470 Valencia (Spain)
alayn.loayssa@unavarra.es; jcapmany@iteam.upv.es*

Abstract: We propose a novel scheme to implement tunable multi-tap complex coefficient filters based on optical single sideband modulation and narrow band optical filtering. A four tap filter is experimentally demonstrated to highlight the enhanced tuning performance provided by complex coefficients. Optical processing is performed by the use of a cascade of four phase-shifted fiber Bragg gratings specifically fabricated for this purpose.

©2008 Optical Society of America

OCIS codes: (999.9999) Single sideband modulation; (070.1170) Analog optical signal processing; (999.9999) Microwave photonics; (999.9999) Microwave optical filters; (999.9999) Transversal filters; (060.3735) Fiber Bragg gratings.

References and links

1. J. Capmany, B. Ortega, D. Pastor, and S. Sales, "Discrete time optical processing of microwave signals," *J. Lightwave Technol.* **23**, 702-723 (2005).
2. R. Minasian, "Photonic Signal Processing of Microwave Signals," *IEEE Trans. Microwave Theory Tech.* **54**, 832-846 (2006).
3. N. You and R. A. Minasian, "A novel tunable microwave optical notch filter," *IEEE Trans. Microwave Theory Tech.* **49**, 2002-2005 (2001).
4. J. Capmany, J. Mora, B. Ortega, and D. Pastor, "Microwave photonic filters using low-cost sources featuring tunability, reconfigurability and negative coefficients," *Opt. Express* **5**, 1412-1417 (2005).
5. B. Vidal, J. L. Corral, and J. Martí, "All-optical WDM multi-tap microwave filter with flat bandpass," *Opt. Express* **14**, 581-586 (2006).
6. A. Loayssa, J. Capmany, M. Sagues, and J. Mora, "Demonstration of Incoherent Microwave Photonic filters with complex coefficients," *IEEE Photon. Tech. Lett.* **18**, 1744-1746 (2006).
7. E. H. W. Chan and R. A. Minasian, "Photonic RF phase shifter and tuneable photonic RF notch filter", *IEEE J. Lightwave Technol.* **24**, 2676-2682 (2006).
8. M. Sagues, A. Loayssa, and J. Capmany, "Multitap complex-coefficient incoherent microwave photonic filters based on stimulated Brillouin scattering," *IEEE Photon. Tech. Lett.* **19**, 1194-1196 (2007).
9. M. Sagues, A. Loayssa, J. Capmany, D. Benito, S. Sales, and R. Garcia Olcina, "Tunable complex-coefficient incoherent microwave photonic filters based on optical single-sideband modulation and narrow-band optical filtering," in *Proc. Optical Fiber Communications Conference (OFC'2007)* paper OWU5.
10. A. Loayssa and F.J. Lahoz, "Broadband RF photonic phase shifter based on stimulated Brillouin scattering and single sideband modulation," *IEEE Photon. Tech. Lett.* **18**, 208-210 (2006).
11. N. K. Berger, B. Levit, B. Fischer, M. Kulishov, D. V. Plant, and J. Azaña, "Temporal differentiation of optical signals using a phase-shifted fiber Bragg grating," *Opt. Express* **15**, 371-381 (2007).
12. A. Loayssa, R. Hernandez, D. Benito, and S. Galech, "Characterization of stimulated Brillouin scattering spectra by use of optical single sideband modulation," *Opt. Lett.* **29**, 638-640 (2004).
13. G. H. Smith, D. Novak, and Z. Ahmed, "Technique for optical SSB generation to overcome dispersion penalties in fibre-radio systems," *Electron. Lett.* **33**, 74-75 (1997).

14. S. Xiao and A. Weiner, "Optical carrier-suppressed single sideband (O-CS-SSB) modulation using a hyperfine blocking filter based on a virtually imaged phased-array (VIPA)," *IEEE Photon. Techn. Lett.* **17**, 1522-1524 (2005).
15. T. Fujiwara and K. Kikushima, "140 Carrier, 20GHz SCM signal transmission across 200km SMF by two-step sideband suppression scheme in optical SSB modulation," in *Proc. Optical Fiber Communications Conference (OFC'2007)* paper OME2 (2007).
16. M. Attygalle, C. Lim, and A. Nirmalathas, "Extending optical transmission distance in fiber wireless links using passive filtering in conjunction with optimized modulation," *IEEE J. Lightwave Technol.* **24**, 1703-1709 (2006).

1. Introduction

Much research has been recently devoted to overcome the inherent limitations of positive-coefficients incoherent microwave photonics filters developing schemes to provide negative and full complex-coefficient filters [1-9]. Tunable complex-coefficient filters have desirable advantages, particularly in terms of tuning, as they provide tunability of their frequency response without altering the spectral shape, basic delay or free spectral range (FSR) [3].

We have recently introduced an all-optical implementation of a two-tap complex-coefficient microwave photonic filter working under incoherent operation [6]. The technique was based on an optically-induced RF phase-shift using optical single-sideband (OSSB) modulation and stimulated Brillouin scattering (SBS) signal processing [10]. Moreover, we have generalized this scheme to built multi-tap complex coefficient filters demonstrating that the technique can be easily scaled [8]. However, these are complex schemes because they require additional devices to generate the optical waves involved and rather high optical powers to pump the nonlinear interaction.

In this work, we introduce another technique to obtain multi-tap complex-coefficient filters, which avoids the inherent complexities of using SBS processing. It is also based on optically processing OSSB modulated signals, but just simple linear optical filtering is needed instead of a nonlinear optical effect. We use a compact implementation that is based on filtering multi-wavelength OSSB signals using a cascade of phase-shifted fiber Bragg gratings (PS-FBG) [11]. This method can be regarded as an evolution of our previously reported two-tap filter which was limited to a single complex coefficient tap [9].

2. Fundamentals of the technique

The key for the implementation of filters with complex coefficients is to obtain a tunable RF phase-shift that remains constant over the microwave spectral region of interest [6-7]. Moreover, this phase-shift must be achieved in the optical domain in order to bypass the bandwidth limitations imposed by the use of electrical circuits. In our technique this is achieved by the combined use of OSSB modulation and narrow band optical filtering. OSSB modulation is deployed because this modulation format provides a correspondence or mapping between the optical and the electrical domains, i.e., with OSSB modulation, variations in amplitude and phase-shift of the optical carrier are directly translated to the conveyed RF signal [12]. If an OSSB modulator is driven by a RF tone $\cos(2\pi f_{RF}t)$ and the optical field at its output is processed to modify only the optical carrier by a factor $A \cdot \exp(j\theta)$, then the detected RF signal in a photodiode is proportional to

$$i(t) = E_{out} \cdot E_{out}^* \propto A \cos(2\pi f_{RF}t - \theta) \quad (1)$$

Therefore, a frequency-independent RF phase-shift can be obtained if we are able to optically phase-shift the optical carrier of an OSSB signal without affecting the modulation sidebands. In our technique we propose the use of PS-FBGs for this purpose. For instance, Fig. 1 displays the experimental characterization of the reflection optical transfer function of a commercial PS-FBG. In addition, it schematically depicts the optical filtering that is to be performed on the OSSB signal in order to generate the RF phase-shift. The optical carrier is

set inside the amplitude notch (surrounded by dotted lines) of the PS-FBG. This is a narrow-band (around 10 GHz in this particular PS-FBG) spectral region of the frequency response where we have an amplitude gap and an associated optical phase-shift. At the same time, the modulation sidebands (simple tone modulation is represented in the figure) fall within the flat amplitude and phase-shift range of the frequency response of the PS-FBG. Tuning the wavelength of the optical carrier we are able to tune the optical carrier's phase-shift, which, as it was explained above, directly translates to the recovered RF signal's phase-shift. A similar tuning could also be obtained shifting the response of the PS-FBG in frequency by changing its temperature or applying strain.

In order to clarify the idea, Fig. 2(a) represents the RF amplitude and phase-shift that, according to Eq. (1), would be recovered as the optical carrier is tuned along the PS-FBG's notch. The traces are obtained by considering ideal OSSB modulation so that the optical spectrum is directly translated to the electrical domain. Figure 2(b) shows that, for this given grating, for frequencies above approximately 10 GHz and below 30 GHz (grey box in Fig. 2(a)) the phase-shift and amplitude can be regarded as frequency independent. Therefore, the bandwidth of the region where we obtain frequency-independent RF phase-shift is limited by two factors: the bandwidth of the amplitude notch and the bandwidth of the flat amplitude and phase-shift region. The former limits the lower RF frequency, while the latter defines the highest RF frequency of operation of the filter. For this particular grating, the attainable phase-shift goes from 0° (tuning the laser at 1540.048 nm) to approximately 250° (1540.1720 nm). Figure 2 also highlights the fact that modifying the wavelength of the optical carrier not only affects its phase-shift, but also alters its mean amplitude. This is due to the fact that we are tuning the laser source along the amplitude notch of the PS-FBG. However, this attenuation can be easily compensated by tuning the power of the laser source at each wavelength.

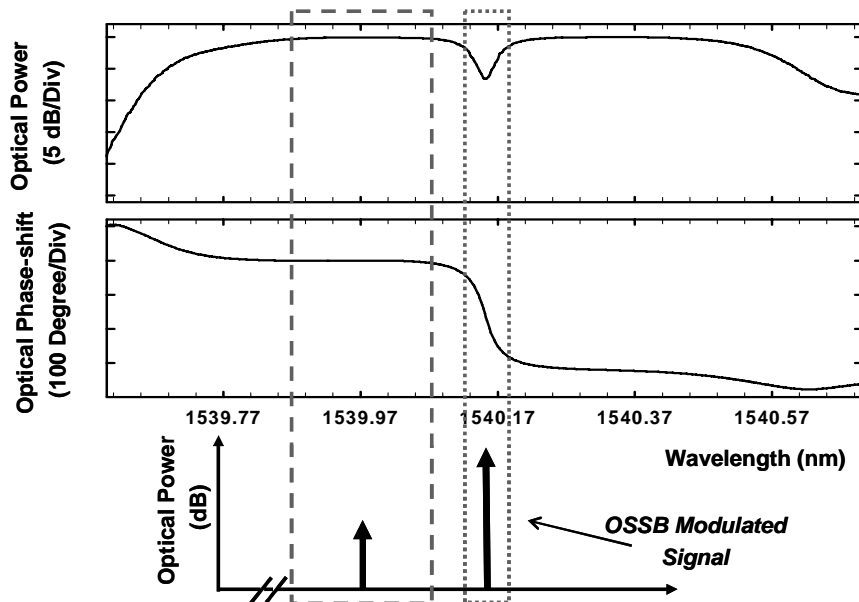


Fig. 1. Fundamentals of the narrow-band optical processing of the OSSB modulated signal using a commercial PS-FBG: Modulation sidebands fall in a linear slope region of the phase spectrum of the PS-FBG, while the optical carrier acquires a differential phase-shift in the notch region.

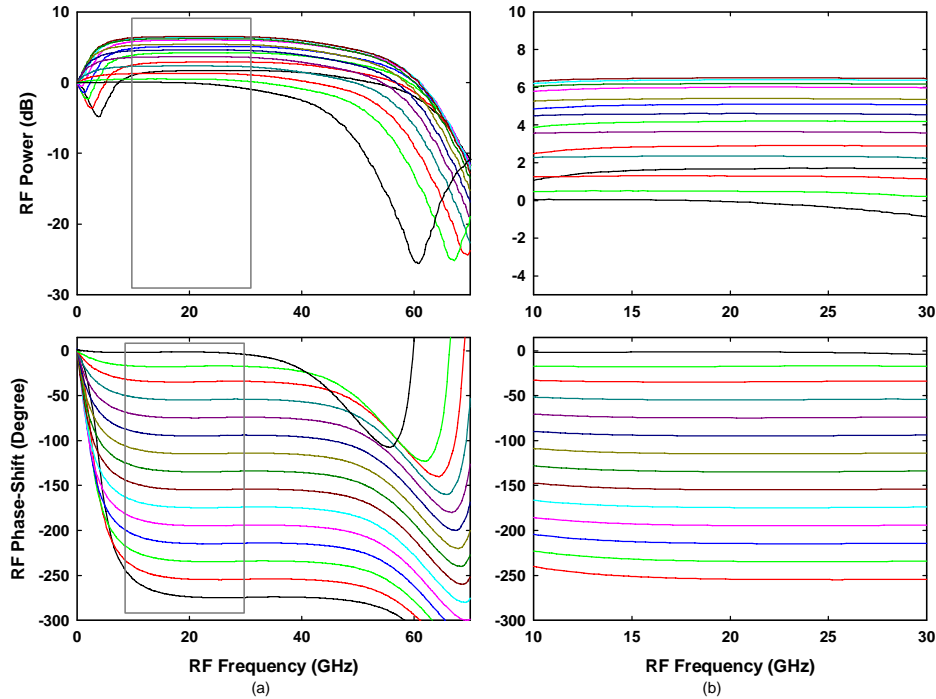


Fig. 2. Representation of the frequency response of the RF photonic phase shifter considering ideal OSSB modulation. (a) Full range, (b) 10 to 30 GHz detail.

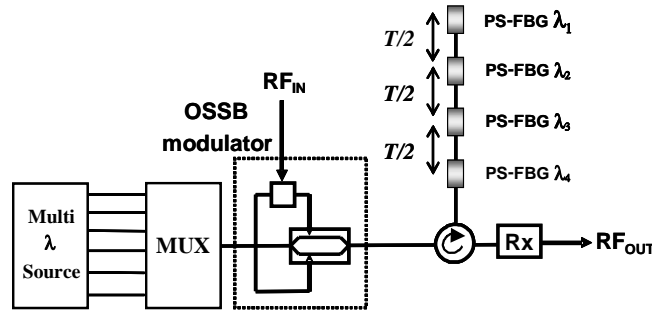


Fig. 3. Experimental setup for the multi tap complex coefficient filter.

3. Multi tap complex-coefficient microwave photonic filter setup

The setup that is needed to implement our proposed multi-tap transversal filter structure is schematically depicted in Fig. 3. An array of tunable laser sources (one per filter tap) is combined and simultaneously modulated using an OSSB modulator that is driven by the RF signal to be processed. In our experiments we use an OSSB modulator based on the 90°-hybrid-coupler method [13]. However, the proposed technique is independent of the OSSB signal generation method. Therefore, other OSSB modulation techniques that are implemented fully in the optical domain could be deployed in order to overcome the bandwidth limitation of the hybrid coupler [14-15]. In our experiment we used a bank of DFB lasers, but for a large number of taps a commercial multi wavelength comb source could be deployed, providing tens of equally spaced spectral lines. Then, the modulated signals are filtered by the combined reflective response of a cascade of PS-FBGs whose central wavelengths match those of the sources. Finally, the filtered RF signal is detected in a broadband optical receiver.

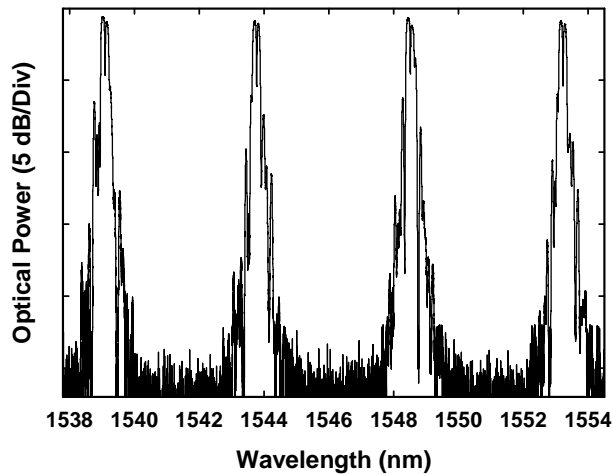


Fig. 4. Reflective amplitude spectral response of the cascade of PS-FBGs.

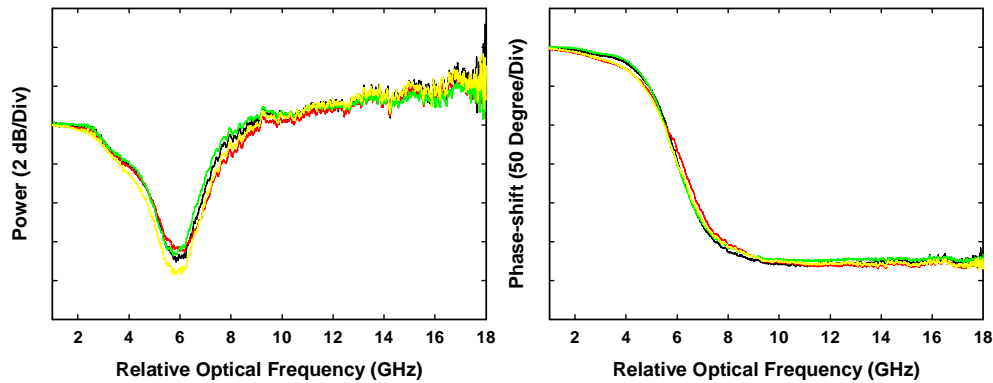


Fig. 5. Spectral characterization of the PS-FBGs.

For our particular experimental demonstration, a total of four PS-FBGs were fabricated in a 14.5 cm length of photosensitive fiber Fibercore PS1250/1500 employing a step by step illuminating process with very accurate phase control. The gaussian beam from an Innova FreD UV laser at 244 nm was focused to $\sim 500 \mu\text{m}$ and four different phase masks were employed (1063.80 nm, 1067.09 nm, 1070.40 nm and 1073.73 nm). Each single PS-FBG was 1 cm long, and the π -phase-shift was created introducing an additional step of length equal to half of the grating period. The 10-pm-resolution spectral response of the reflection of the grating cascade is shown in Fig. 4. The central wavelengths of the gratings were 1539.0940 nm, 1543.7740 nm, 1548.5120 nm and 1553.2220 nm.

Our goal was to fabricate four PS-FBGs with very similar reflective amplitude and phase-shift frequency response shape, each one centered in a different wavelength. Figure 5 shows the optical amplitude and phase-shift characterization of the reflection transfer function of the four PS-FBGs using the OSSB technique [12]. The optical frequency axis has been normalized so that the notches of the four PS-FBGs are aligned in the figure, showing a very good match between the responses of the gratings. The RF bandwidth of the measurement was limited to 18 GHz by the bandwidth of the deployed OSSB modulator. The small ripple in the

measurement is attributed to the quality of the deployed OSSB signal whose unwanted sideband suppression was around 20 dB for the worst case frequency.

The gratings were spatially separated along the fiber at 4.5 cm intervals. This separation provides the basic delay T of the transversal filter and hence it defines its FSR, which in this case was 2.27 GHz. In order to verify that the spacing between gratings was constant, we measured the delay of an optical signal traveling between them using the setup in Fig. 3. This is done by setting a tunable laser source in the flat amplitude region of the gratings, and measuring the electrical delay using an electrical vector network analyzer. The results are shown in Fig. 6, showing that the relation between these measured electrical delays is almost linear as expected for a constant spacing between the gratings.

4. Experimental results

First, we show the feasibility of the proposed scheme to obtain a frequency-independent RF phase-shift for a given range of RF frequencies. Figure 7 shows the recovered RF signal's phase-shift and amplitude frequency response for the PS-FBGs centered around 1539.0940 nm measured using the setup in Fig. 3 with just one laser enabled, whose wavelength is tuned from 1539.12 nm to 1539.06 nm. As it was shown above, the low frequency operation of the RF phase-shifter is limited by the linewidth of the PS-FBG notch, which in this case is around 5 GHz. On the other hand, the higher usable frequency is limited by the bandwidth of the flat phase-shift spectral region of the PS-FBG to approximately 8 GHz.

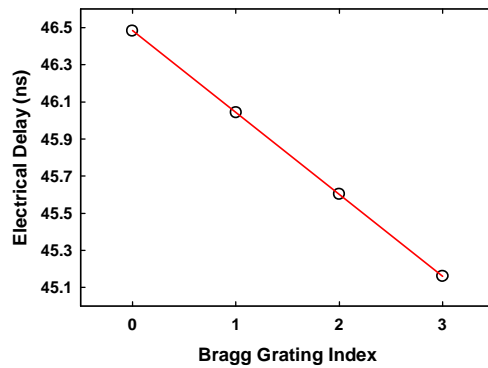


Fig. 6. Measured electrical delay for each PS-FBG (symbols).

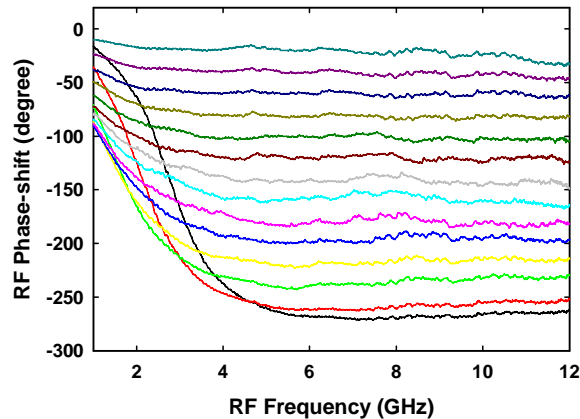


Fig. 7. Frequency response of the RF photonic phase-shifter.

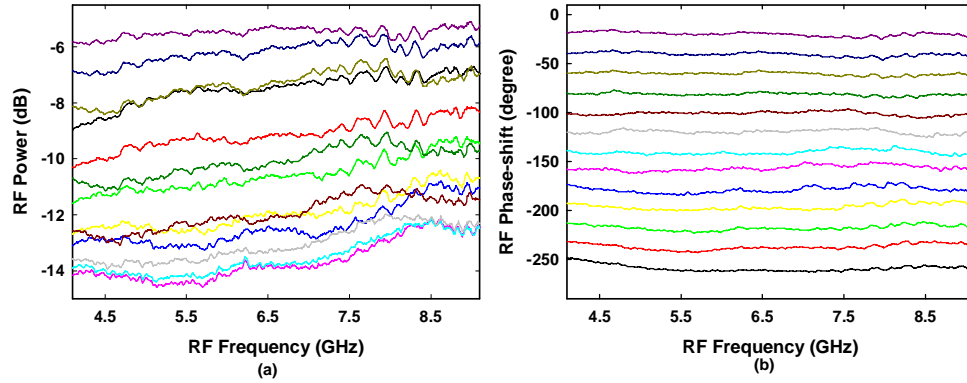


Fig. 8. Measured (a) amplitude and (b) RF phase-shift for one of the PS-FBGs for different wavelengths of a laser source.

Figure 8 shows a closer look to that range of frequencies showing that the phase-shift and the amplitude of the recovered RF signal can be regarded as frequency independent. However, a difference in the relative ripple among the traces can be observed. This small ripple (< 1 dB) is attributed to the residual sideband in the deployed OSSB signal. This particular grating provides a maximum phase-shift of approximately 250° . Therefore, cascading two of them we should be able to achieve more than the required 360° needed to implement any complex-coefficient tap. Figure 8(a) shows that as we tune the wavelength of the optical carrier along the notch of the PS-FBG, both the phase-shift and the mean amplitude of the recovered RF signal are modified. In addition, this attenuation would be even greater if two gratings were cascaded in order to achieve the full 360° range. However, this attenuation can be easily compensated by tuning the power of the laser sources at each wavelength. Furthermore, attenuation of the optical carrier has been found to be a convenient method to enhance the modulation depth and improve the noise figure and dynamic range of optical links [16]. Therefore, the control of two independent parameters (laser wavelength and power) is required in order to tune the phase-shift for each tap of the filter. In order to reduce the impact of this power reduction in practical implementations of the filter, future work should focus on the fabrication of PS-FBGs with higher phase-shifts and lower attenuation in the center of the notch.

Finally, we experimentally demonstrate a four-tap complex-coefficient filter. In order to highlight the enhanced flexibility in the synthesis of frequency responses given by complex coefficients we have focused the experiments on one of the main features provided by them: tuning of the spectral response of the filter without altering its shape or FSR [6]. Consider an N -tap transversal filter whose frequency response is given by

$$H(e^{j\omega T}) = \sum_{n=0}^{N-1} a_n e^{-j\omega T n} \quad (2)$$

where a_n are the filter taps coefficients. If we wanted to tune the response of such a filter by shifting its central frequency by a factor ω_0 without changing the free spectral range or the shape of the filter we would end up with a new frequency response

$$H_s(e^{j\omega T}) = H(e^{j(\omega-\omega_0)T}) = \sum_{n=0}^{N-1} a_n e^{-j\omega_0 T n} e^{-j\omega T n} \quad (3)$$

Therefore, tuning of the frequency response of a transversal filter requires complex-coefficient taps with phase-shifts given by $n\omega_0 T$.

As it is shown in Fig. 8(b), the maximum phase-shift of our complex coefficients is limited to approximately 250° . This leads to a continuously tuning range of the filter of approximately $\text{FSR}/4.36$ (3). As mentioned above, this limitation would be overcome if two PS-FBGs are cascaded to implement each coefficient. Figure 9(a) displays the frequency response of the complex coefficient transversal filter when all its coefficients are positive and of equal amplitude. Figure 9(b) and Fig. 9(c) show the tuning of this response in $\pm\text{FSR}/4.36$ frequency shifts by appropriately setting the complex coefficients to $a_n = e^{\pm jn2\pi(250/360)}$, where n is the tap number (3). Experimental measurements (symbols) show excellent agreement with theoretical calculations (solid line). Frequency response of the filter with all positive coefficients is also shown (dashed line). As expected from Eq. (3), the FSR and the shape of the filter are not altered when its frequency response is tuned.

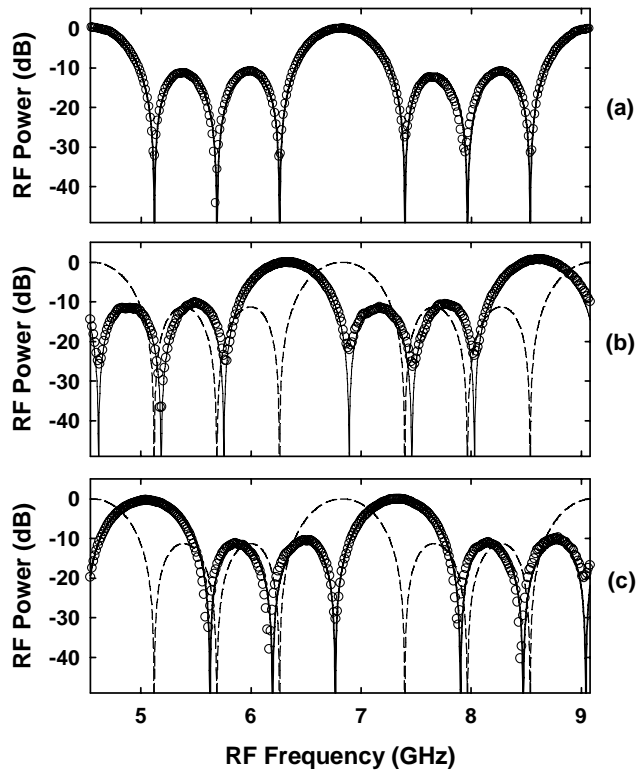


Fig. 9. Frequency response of the four-tap complex coefficient filter.

5. Conclusions

A novel technique based on OSSB modulation and PS-FBGs for the implementation of complex-coefficient microwave photonic filters has been demonstrated. A simple four-tap filter has been used to demonstrate the principles of the technique, but the same processing can be easily extended to filters with arbitrary number of coefficients. Moreover, it has been found that PS-FBGs with narrower notch and broader flat region must be used if broader frequency operation is desired. In addition, further work should focus on the fabrication of PS-FBGs with larger phase-shifts and in the developing of schemes where PS-FBGs are cascaded in order to achieve full FSR tunability. However, the technique is not limited to optical filtering using PS-FBGs and could be deployed with any optical device which can filter the phase-shift of the optical carrier without affecting the sidebands of the OSSB signal.

Acknowledgments

This work was supported by the Plan Nacional I+D+I through projects TEC2007-67987-C02-02/MIC and TEC2007-68065-C03-01, and by the Gobierno de Navarra through the research project 13.326.